Acc. Miscell. S. Sauv

ISR-VAC/66-11
revised
15th December, 1966

MONTE CARLO COMPUTATIONS ON MOLECULAR FLOW IN PUMPING SPEED TEST DOMES

by

E. Fischer and H. Mommsen*

1. INTRODUCTION

The ISR Vacuum Group at CERN uses for pumping speed measurements a test dome as proposed by R. Calder and as shown in Fig. 1. It is a variant of the well-known two-gauge-and-calibrated-orifice method (Barre et al. 1956). The diameter of the dome is equal to that of the pump throat. Its length between orifice and pump flange is three times the diameter. For a dome of 6 inch diameter the conductance of the orifice is about 8 ℓ/s. The gauge measuring P_1 has a distance from the flange of two thirds of the pump throat diameter and is arranged as pressure converter (also called transducer). The pressure converter measures directly a pressure, but indirectly the collision rate of molecules against the wall of the test dome. It "converts" collision rates into pressure. It appears that the idea of the pressure converter has first been proposed by Buhl and Trendelenburg (1965). Our converter can be regarded as a simplified version of Buhl's more elaborate spherical pressure converter.

The purpose of this - as of any other - test dome is to measure the so-called "intrinsic" pumping speed (also called "true" pumping speed, or "large dome" pumping speed). It is defined as the speed one would measure if the pump were connected by its flange directly, that is without tubulation, to a volume which is large compared to the pump diameter and if the gauge were sufficiently far away from

---

*) Permanent address: Institut für Strahlen- und Kernphysik der Universität Bonn, Germany.

the pump. The speed would then be simply given by

$$S = Q/P \,. \qquad (1)$$

Several authors (Stickney and Dayton 1963, Nöller 1963, Steckelmacher 1963) have discussed the errors made by measuring pumping speeds by means of a tubular test dome and proposed corrections. Only recently (Buhl and Trendelenburg 1965, Dayton 1965, Steckelmacher 1965 a und b, Chubb 1966) the idea appeared that for a given test dome such a gauge position can be found that the measured pressure is equal to the pressure one would measure in an ideal, that is sufficiently large test dome and that, consequently, Eq. (1) could be applied for the tubular test dome as well. W. Steckelmacher published a graph (1965 b) indicating the "ideal" position for gauges in dependence of the height of the test dome. The gauge position of the CERN test dome has been chosen from this graph.

The present paper presents the results of a study carried out at CERN on the fast electronic computer CDC 6600 in order to check the choice of gauge position and to investigate furthermore the influence of the pump geometry. A so-called Monte Carlo programme has been used which simulates the random motion of many individual molecules inside the dome from wall collision to wall collision until they are absorbed by the pump. By simply counting the wall collisions for different zones, the programme predicts the variation of the wall collision rate along the dome. This has been the main reason for arranging the gauge P_1 as converter: The wall collision rate, which, in spite of the non-equilibrium condition, is easy to measure by a converter is also easy to calculate by a Monte Carlo computer programme.

2. GENERAL RELATIONSHIPS

The conditions in the top volume are close to a Maxwell-Boltzmann equilibrium, because the diameter of the orifice is much smaller than

the dome diameter. In the programme, therefore, the molecules are made to enter the lower dome at random, but so that they follow a cosine distribution law. Also the reflection from the cylinder wall and from the orifice plate is randomized in a cosine distribution.

A possible representation for a pump is a pumping probability α in the plane of the bottom flange of the dome. If a molecule reaches this plane it is absorbed at random or reflected but so that on the average the fraction of absorbed molecules equals α. In the simplest pump representation which we call (a) the reflected molecules follow the cosine law. This is strictly valid only for an ideal cryopump with its pumping surface in the plane of the bottom flange of the dome. The pumping probability is in this case identical with the sticking coefficient. In a getter ion pump, for instance, the pumping takes place at some distance from the pump flange and there is a passive tubulation between pumping surfaces and pump flange. In this case, the reflected molecules crossing the flange plane have angles with respect to the axis which are not distributed in a cosine law. Therefore, other more realistic pump representations have also been used for computations. The result is, however, as will be shown, that the influence of the distorted angular distribution on a pumping speed measurement is only small, so that the pump representation (a) is for all pumps a sufficiently good approximation.

The programme registers all wall collisions and stops when their number exceeds a present value, usually one million. Then the axial co-ordinates of all wall collisions are presented in the form of a histogram with chosen resolution. The obtained histograms are proportional to the collision rate density as function of the axial co-ordinate.

For reasons of normalization the axial co-ordinate x is replaced by the dimensionless co-ordinate $X = x/R$, where R is the radius of pump throat and test dome. X is zero at the orifice.

It has now to be shown how the value of the histogram at X is related to the pressure $P_1(X)$ measured in a converter situated at X.

Let N be the total number of injected molecules and Z(X) the number of registered collisions in a zone. The computed probability that an injected molecule hits this zone is Z(X)/N. Let ΔX be the resolution of the histogram. The width of the equivalent zone is $R\Delta X$ and its surface area $2\pi R^2 \Delta X$.

The predicted collision rate density $\nu(X)$ (in molecules per second and square metre) at the distance X is Q the number of molecules injected into the real test dome per second multiplied by the probability Z(X)/N, divided by the surface area $2\pi R^2 \Delta X$

$$\nu(X) = \frac{Q\, Z(X)/N}{2\pi R^2 \Delta X} . \qquad (2)$$

The gas flow Q (in sec^{-1}) from the top volume is simply given by

$$Q = A\, P_2\, C(M, T) \qquad (3)$$

where A is the area of the orifice, P_2 the pressure in the top volume and C a gas kinetic factor depending on the molecular mass M and the temperature T.

There is also a Maxwell-Boltzmann equilibrium inside the converter. Hence, the relationship between the collision rate $\nu(X)$ and the measured pressure $P_1(X)$ is

$$\nu(X) = P_1(X)\, C(M, T) \qquad (4)$$

in analogy to Eq. (3). At constant flow as many molecules enter the converter as leave it. From Eqs. (2), (3) and (4) one obtains

$$P_1(X) = P_2 \frac{A}{\pi R^2} \frac{Z(X)}{2\, N \Delta X} . \qquad (5)$$

The programme computes directly the function

$$D(X) = Z(X)/2\ N\Delta X \ . \qquad (6)$$

This computed distribution function makes it possible to predict which pressure one will measure in a converter at distance X from the orifice and for a given set of parameters like dome height and pumping probability, namely

$$P_1(X) = P_2 \frac{A}{\pi R^2} D(X) \ . \qquad (7)$$

For a direct measurement of the intrinsic pumping speed one could hypothetically replace the bottom volume of the CERN test dome by a large volume and however maintain the top volume and the injection orifice. One would then measure in the large dome a pressure

$$P_1 = P_2 \frac{A}{\pi R^2} \frac{1}{\alpha} \qquad (8)$$

as can be easily seen. Hence, the value D as defined by Eq. (7) would be

$$D = 1/\alpha \ . \qquad (9)$$

Consequently, the "ideal" gauge position is the X_i, for which

$$D(X_i) = 1/\alpha \ . \qquad (10)$$

3. RESULTS

3.1 Pump representation (a)

This representation is characterized by a pumping probability α in the plane of the pump flange and a cosine distribution of the reflected molecules.

Figure 2 shows the computed functions D(X) for a test dome of a height of 6 R in the interval $3.0 \leq X \leq 6.0$ that is in the lower half of the dome. The parameter is the pumping probability α. The resolution of the histogram is 0.5. The original step function (see top curve) has been smoothed out by connecting the midpoints of all intervals by straight lines. The gauge position on the CERN test dome (Fig. 1) is $X_G = 4.67$. Therefore, $1/D(X_G)$ for $X_G = 4.67$ has been plotted in Fig. 3 as function of α. $1/D(X)$ has been plotted instead of D(X), because in this way the curve becomes approximately a straight line and is easier to interpolate.

With the help of this curve the intrinsic pumping speed can be determined in the following way: From the radius R, the orifice area A and the measured pressures P_2 and $P_1(X_G)$ one calculates

$$1/D(X_G) = \frac{P_2 \, A}{P_1(X_G) \, \pi R^2} . \qquad (11)$$

With this, one finds from Fig. 3 the corresponding α, from which the speed in ℓ/s is obtained straightforward from the equation

$$S = \alpha \, 3.64 \, \pi R^2 \sqrt{T/M} . \qquad (12)$$

The pumping speed is calculated from the ratio of the two measured pressures (Eq. (11)). It is essential that both gauges have the same sensitivity or that the ratio of their sensitivities is known. For this purpose a second gas injection valve and nozzle have been installed on the test dome closely to the pump (see Fig. 1). By injection through this valve the ratio of the sensitivities of the two gauges can be measured over the whole measuring range and for the gas the speed of which will be measured. For pumping speed measurements on getter ion pumps there exists another method of gauge comparison: one can switch off the pump electrically and inject the gas in small portions through the top injection valve and read

the pressure in between under static conditions. In this case there is no need for the lower injection nozzle. It can be eliminated if one is afraid that this obstacle to molecular flow influences the speed measurements.

If the gauge position is the "ideal" one as defined before, one can also determine the intrinsic pumping speed from the conventional equation

$$S = Q/P_1 \qquad (1)$$

or (Barre et al. 1953)

$$S = C_o\left(\frac{P_2}{P_1} - 1\right) \qquad (13)$$

where C_o is the molecular conductance of the injection orifice.

As one can see $X_G = 4.67$ is almost the ideal gauge position but not exactly. Otherwise all measured points would lie on the straight line $1/D(X_G) = \alpha$. In order to find out what the ideal gauge position would be, we added to the curves in Fig. 2 horizontal lines at distance $1/\alpha$ from the X-axis. Where such a line for a given α intersects with the corresponding curve, there is the ideal gauge position, because there is

$$D(X_G) = 1/\alpha \; . \qquad (10)$$

All intersection points are combined by a dashed line. One recognizes that there is a certain dependence of the ideal gauge position on α, though not a strong one. For pumping probabilities between 0.5 and 1.0, the ideal gauge position is 0.59 diameter above the flange ($X_G = 4.82$). For $\alpha = 0.3$ the ideal position is almost exactly 2/3 diameter ($X_G = 4.67$) as on the CERN test dome. For $\alpha = 0.2$ the ideal distance would be 3/4 diameter. Getter ion pumps have typically a

pumping probability between 0.2 and 0.3. The chosen gauge position at 2/3 diameter is, therefore, a good choice for getter ion pumps. The errors are never important. Table I shows the error made in a pumping speed measurement as function of α. Except for $\alpha = 0.2$ all measured speeds are smaller than the true ones.

Table I

Relative error in pumping speed measurement with gauge at X = 4.67

α	ΔS
0.2	+ 1.6 %
0.3	- 0.3 %
0.4	- 1.6 %
0.5	- 4 %
0.6	- 4 %
0.7	- 4 %
0.8	- 5 %
0.9	- 6 %
1.0	- 8 %

It should, however, be emphasized that there is no real necessity to place the gauge on an "ideal" position. For any gauge position a graph of $1/D(X_G)$ can be established as function of α and the pumping speed be determined with its help.

3.2 Pump representation (b)

It is a valid argument against the described method of pumping speed measurement that in many pumps, like getter ion pumps, the pumping action takes place at some distance from the pump flange. As a result of this the molecules re-entering the dome from the pump side

have no cosine distribution as assumed in representation (a).

The computer programme has therefore been modified for a different pump representation, called (b) as shown schematically in Fig. 4.

The pumping action takes place at a distance L_p from the flange. In this plane molecules are absorbed by a pumping probability α_o and otherwise reflected in a cosine law. The dome itself and the injection into it remain unchanged.

The programme computes as function of α_o and L_p two new values, α and F. α is the pumping probability for the pump flange. F is a factor characterizing how much the angular distribution of the backstreaming molecules deviates from a cosine distribution. This factor has to be defined.

A cosine distribution is normally described by the equation

$$\frac{1}{N}\frac{dn}{d\omega} = \frac{1}{\pi}\cos\Theta \qquad (14)$$

where Θ is the angle between the axis of the dome and the direction of a reflected molecule and ω the solid angle. Equation (14) can also be written in the form

$$\frac{1}{N}\frac{dn}{d\Theta} = \sin 2\Theta \qquad (15)$$

which is more convenient in our case.

Figure 5 shows as an example the computed angular distribution for $\alpha_o = 0.7$ and $L_p = 2.0$ R. The resolution of the histogram is $\pi/20$. The dashed histogram is obtained by averaging the function $\sin 2\Theta$ (Eq. (15)) over the same intervals. The integral over each of the histograms is unity. The easiest way of expressing the deviation from the sine function is by determining the coefficient

of the next term of a Fourier series.

$$\frac{1}{N}\frac{dn}{d\vartheta} = \sin 2\vartheta + F \sin 4\vartheta \; . \qquad (16)$$

This is equivalent to

$$\frac{1}{N}\frac{dn}{d\omega} = \frac{1}{\pi}\cos\vartheta\,(1 + 2F\cos 2\vartheta) \qquad (17)$$

if one differentiates with respect the solid angle ω as in Eq. (14).

A subroutine of the computer programme finds by using a "least square fit" the coefficient F which matches best the given computed distribution. For the example of Fig. 5 F = -0.189. The minus sign indicates that small angles ϑ ($< \pi/4$) occur less frequently than large ones ($> \pi/4$). This is exactly the opposite of the angular distribution of a molecular flow out of a long tube. In the latter case F is positive. The factor F is called "beaming factor".

At the bottom of Fig. 5 is traced to the left the undisturbed cosine distribution in the conventional presentation as polar diagram and to the right the distorted polar diagram as calculated from the computed histogram of the example from Fig. 5.

Figure 6 shows the computed beaming factor F as function of the basic pumping probability α_o for different length L_p of the passive pump neck. The statistical errors are relatively large as indicated. The highest distortion is found for $\alpha_o = 1.0$ and $L_p = 2.0$ with $F = -0.29$.

Figure 7 shows the computed α as function of α_o and L_p. This graph is first of all of practical value. It is often the case that a pump is connected to a large tank over a more or less short tubulation of the same diameter as the pump throat. From the graph one can find out, what the effective speed at the tank wall will be. Secondly, the graph allows comparisons with the results of other

workers. The values of α (α_o = 1, L_p) at the right border, for instance, are nothing else but the well-known and often computed Clausing factors. The agreement within the statistical limits is good and gives confidence in the validity of our programme.

3.3 Pump representation (c)

In most titanium sputter ion pumps the pumping action takes place in longitudinal slits arranged around a central duct in prolongation of the pump neck. Figure 8 shows the scheme of a representation which describes better this geometry. The basic pumping probability α_o is the average over the high pumping probability at the entrance of the slits and the passive walls inbetween. Only one example of this scheme with an active pump length of 5R and a passive neck of 2R (taken from a pump actually on the market) has been put into the programme. α_o has been varied between 0.05 and 0.60.

Figure 9 shows as result the plot of the beaming factor F and the pumping probability α for the pump flange as function of the basic pumping probability α_o. For a pump with α = 0.5 F is -0.25. Chosing from representation (b) the pump with a neck of 2R and an α of also 0.5, we find almost exactly the same beaming factor of -0.25. It seems that this factor depends essentially only on α and the length of the passive pump neck.

For pump representation (b) α is always smaller than α_o, not so for representation (c). For α_o = 0.1, for instance, α is even larger than 0.3. This is the result of the so-called "maze" effect. A molecule, once it has entered the active pumping zone has in the average several times the chance of being absorbed before it leaves the active zone. Hence, the total pumping probability α can very well be larger than the basic pumping probability α_o.

3.4 Pump representation (d)

The question is now, how a negative beaming factor of the order as found for the pump representation (b) and (c) influences the

function D(X) and the ideal gauge position as computed for pump representation (a). The programme for representation (a) has, therefore, been modified in the sense that the molecules which are reflected from the pump do not follow any more the cosine law but have a distribution function according to

$$\frac{1}{N}\frac{dn}{d\Theta} = \sin 2\Theta + F \sin 4\Theta \, . \qquad (16)$$

Only one extreme case with F = -0.24 has been computed. The result is that the influence of a negative beaming factor of this order is only very small. This can be seen from Table II, which shows the values of $D(X_G, F)$ for $X_G = 4.67$ and for F = 0 and -0.24 in dependence on the pumping probability α.

Table II

The influence of the beaming factor
on the pressure measurement
$X_G = 4.67$

α	$D(X_G, F = 0)$	$D(X_G, F = -0.24)$	Difference in %
0.15	6.465	6.370	- 1.5
0.20	4.998	4.806	- 3.8
0.25	4.018	3.843	- 4.3
0.30	3.419	3.339	- 2.3
0.35	2.937	2.837	- 3.4
0.40	2.561	2.484	- 3.0
0.45	2.297	2.271	- 1.1
0.50	2.064	2.022	- 2.0

The deviation is such that for a pump with a negative beaming factor the pressure measured at given gauge position is smaller than for a pump without beaming factor. Hence, the obtained pumping speed is greater than the true one.

3.5 ISO test dome

The International Standard Organisation (ISO) has proposed in 1965 (ISO/TC 112 (Secretariat - 8) 8) a pumping speed test dome for diffusion pumps with a height of three pump throat radii. We applied our programme also to such a dome, primarily in order to check whether the proposed gauge psotion of 1.2 R distance from the flange is close to the ideal one. The results of the computation based on pump representation (a) are presented in Table III.

Table III

Ideal gauge position for a test dome with the height of 3 R

α	distance from flange
0.2	1.33 R
0.3	1.15 R
0.4	1.13 R
0.5	1.10 R
0.6	1.05 R
0.7	1.09 R
0.8	1.05 R
0.9	1.04 R
1.0	1.09 R

There is a slight statistical scattering of the data, but one recognizes the same typical dependence of the ideal gauge position on the pumping probability α as found for the 6 R test dome. For diffusion pumps with $0.3 \leq \alpha \leq 0.6$ a compromise would be a position around 1.1 R. From W. Steckelmacher's analytical work (1965 b) one would predict 1.14 R.

J. Chubb (1966) applied his own Monte Carlo computer programme to the ISO test dome assuming a gauge position of 1.2 R distance from the flange. Figure 10 compares Chubbs results with our own. On the diagram 1/D (1.2) is plotted as function of α as in Fig. 3. The squares are the points computed by Chubb (Fig. 11 of his report). It should be noted that Chubb calls 1/D the "apparent sticking coefficient". The circles are our own results. The difference is first of all not important and can secondly be fully explained by the differences in pump representation. Chubb put into his programme a realistic representation for a diffusion pump with a passive neck and a passive top cap, while we had used the simple pump representation (a). In Chubb's representation the reflected molecules must have a certain negative beaming factor which decreases $D(X_G)$ as we have seen with pump representation (d) and increases $1/D(X_G)$. So it comes that Chubb found 1.2 R to be the ideal position, while our (less realistic) computations lead to 1.1 R. But - it must be said again - the difference is negligeable for all practical purposes.

REFERENCES

R. Barre, G. Mongodin and F. Prevot, 1956:
Le Vide, 11, 25 (1956),
Une méthode absolue de mesure des vitesses de pompage en régime moléculaire.

R. Buhl, E.A. Trendelenburg, 1965:
Vacuum, 15, 5 (1965),
Avoiding systematic errors in measuring the pumping speed of high vacuum pumps.

J.N. Chubb, 1966:
UKAEA, Culham Laboratory Report CLM-R54 (1966),
A Monte Carlo computer programme for analysis of molecular gas flow.

B.B. Dayton, 1965:
Vacuum, 15, 53 (1965),
The measured speed of an "ideal pump".

H.G. Nöller, 1963:
Vacuum, 13, 539 (1963),
The problem of specially large systematic errors in the measurement of pumping speeds of high vacuum pumps of large output.

W. Steckelmacher, 1964:
Vacuum, 14, 103 (1964),
Comment on "The problem of large systematic errors in the measurement of pumping speeds of high vacuum pumps".

W. Steckelmacher, 1965 a:
Vacuum, 15, 249 (1965),
The measurement of the speed of pumps.

W. Steckelmacher, 1965 b:
Vacuum, 15, 305 (1965),
Some comments on "The measurement of the speed of pumps".

W.W. Stickney, B.B. Dayton, 1963:
American Vacuum Symposium Transactions 1963, p. 105.
The measurement of the speed of cryopumps.

Several contributions in close relationship to the subject of the present report have been presented at the Conference on the Performance Assessment of High Vacuum Pumps held at the University of Sussex on 19-21 April, 1966, and will soon be published in Vacuum:

B.L. Bates, L. Laurenson and W. Steckelmacher:
Effect on the measured pumping speed of a diffusion pump of the test head size and the position of the pressure gauge and air inlet.

R. Buhl:
Pressure measurement for determination of the speed of high vacuum pumps.

J.N. Chubb:
Monte Carlo analysis of pumping speed test dome performance for several vapour diffusion pump geometries.

W. Steckelmacher:
Review of the molecular flow conductance for systems of tubes and components and the measurement of pumping speed.

H.G. Nöller:
Evaluation of high vacuum pumps.

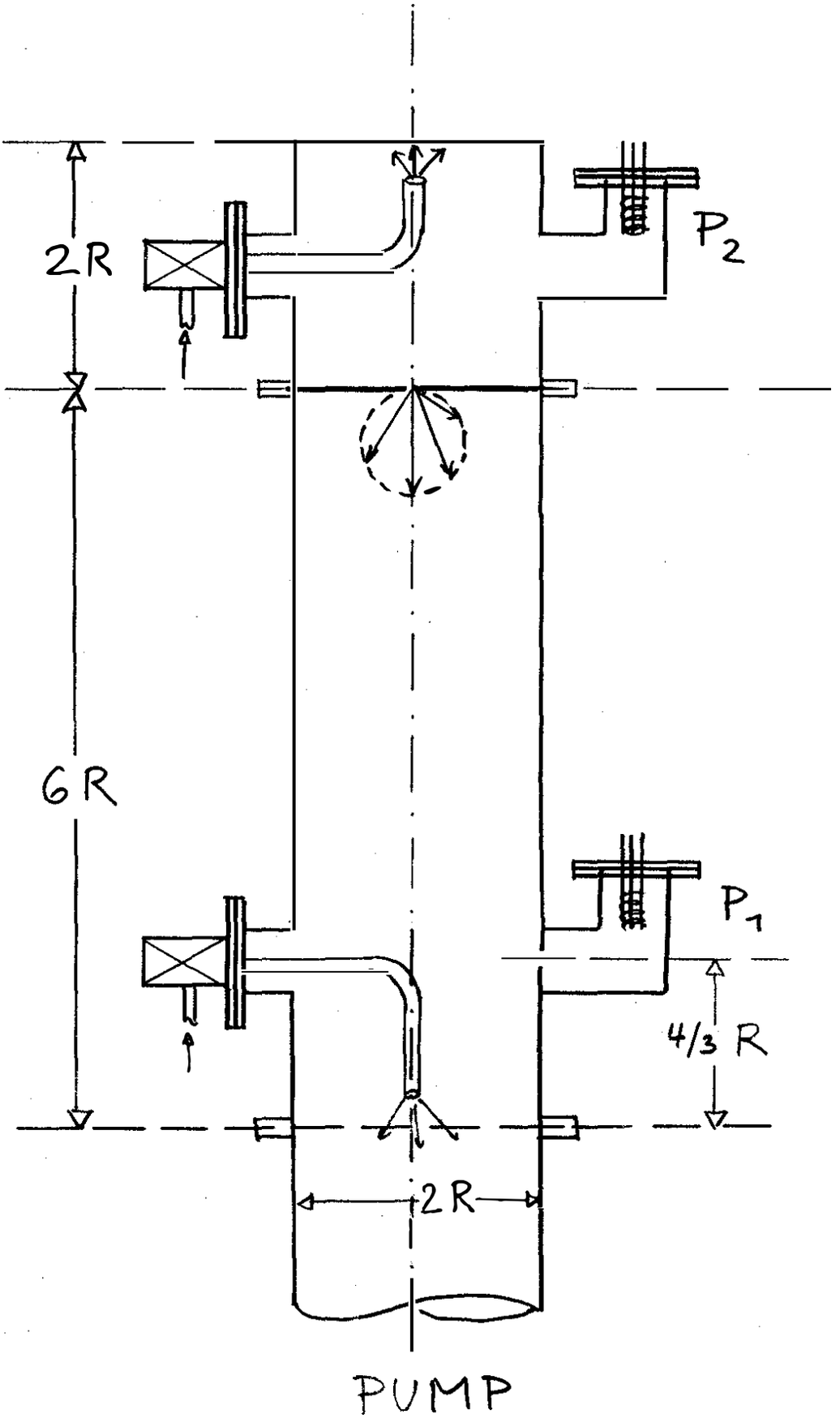

Fig. 1 CERN test dome 6R

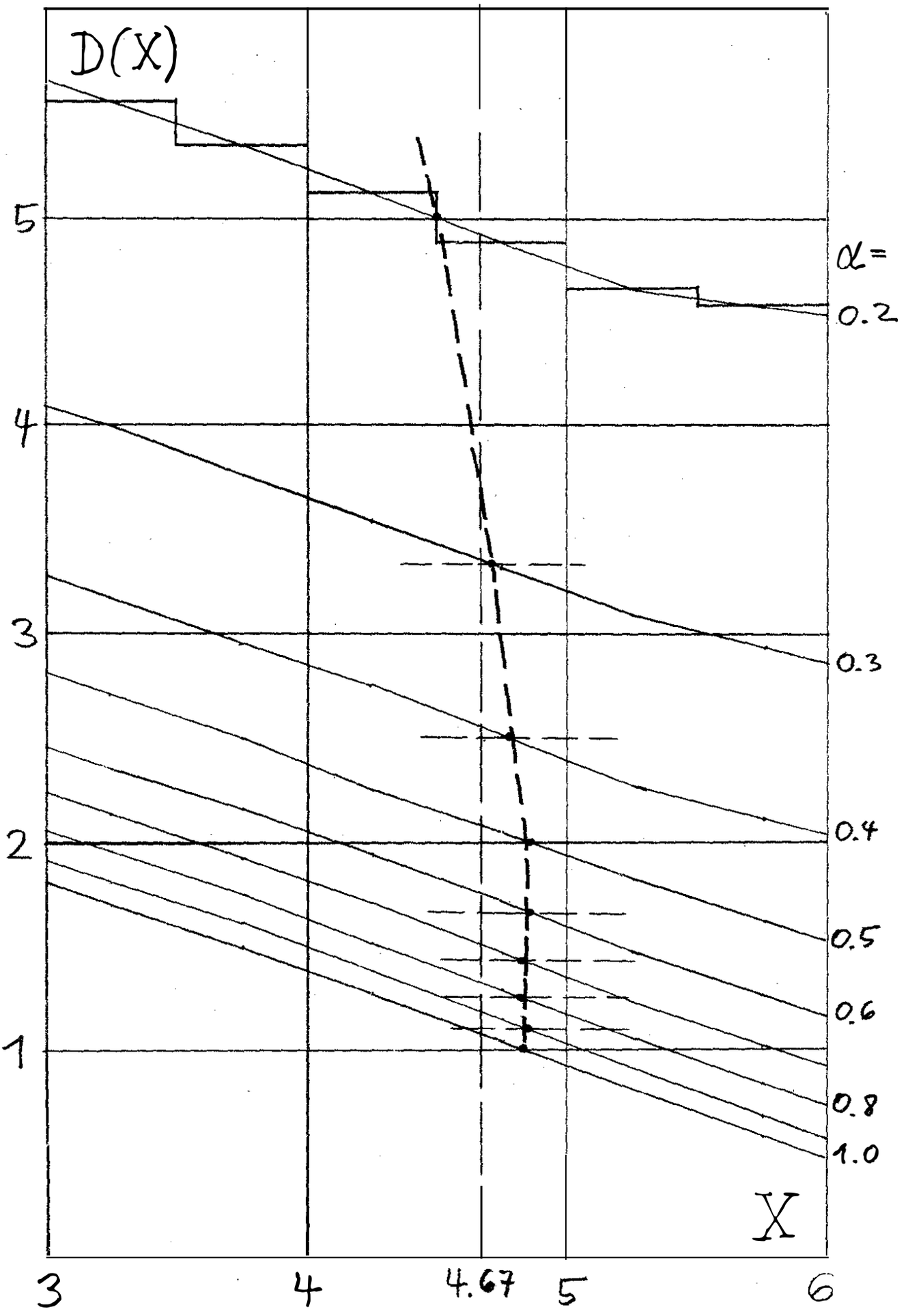

Fig. 2 $D(X,\alpha)$ for pump representation (a)

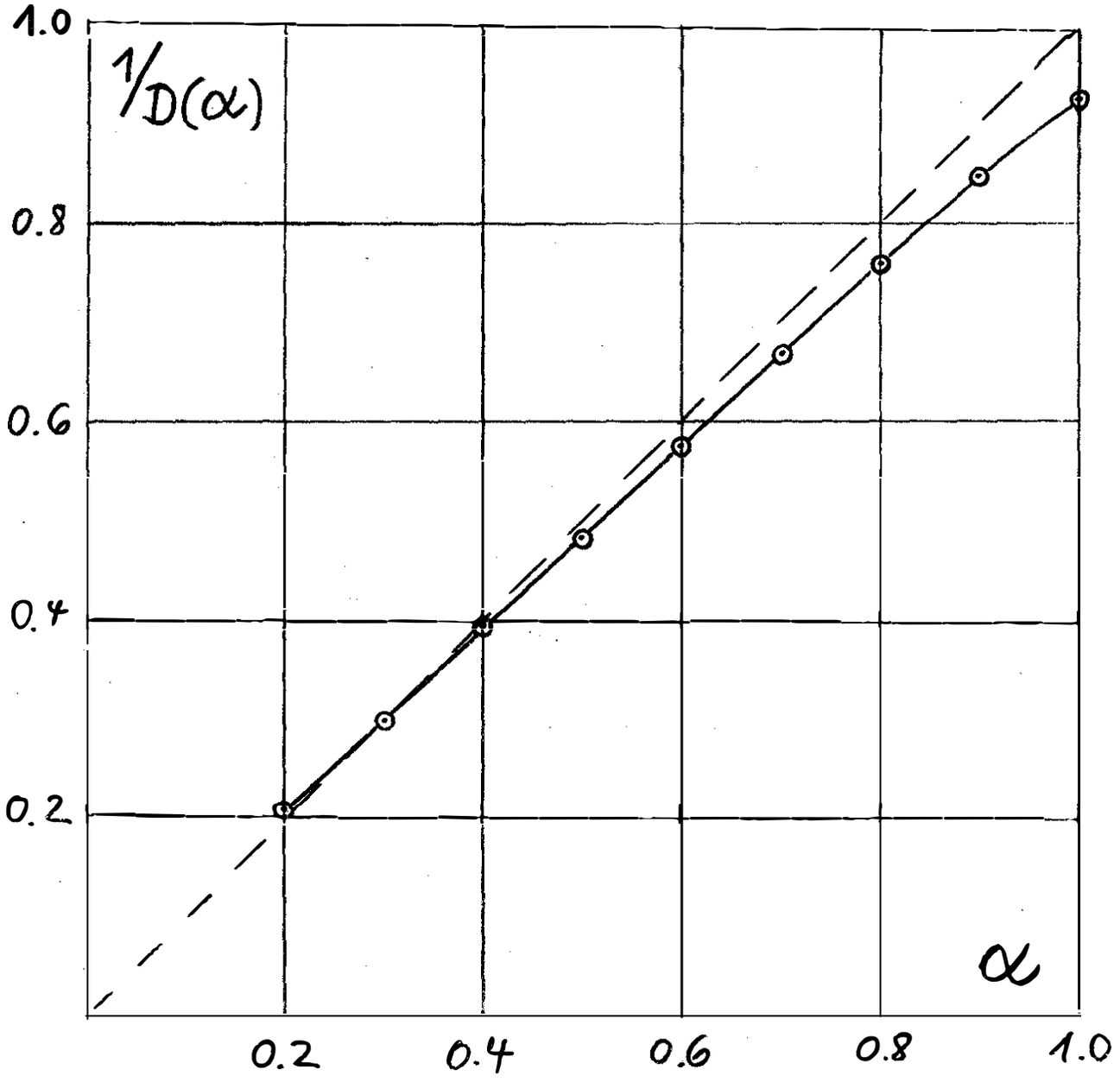

Fig. 3 $1/D(\alpha)$ for $X_G = 4.67$ for pump representation (a)

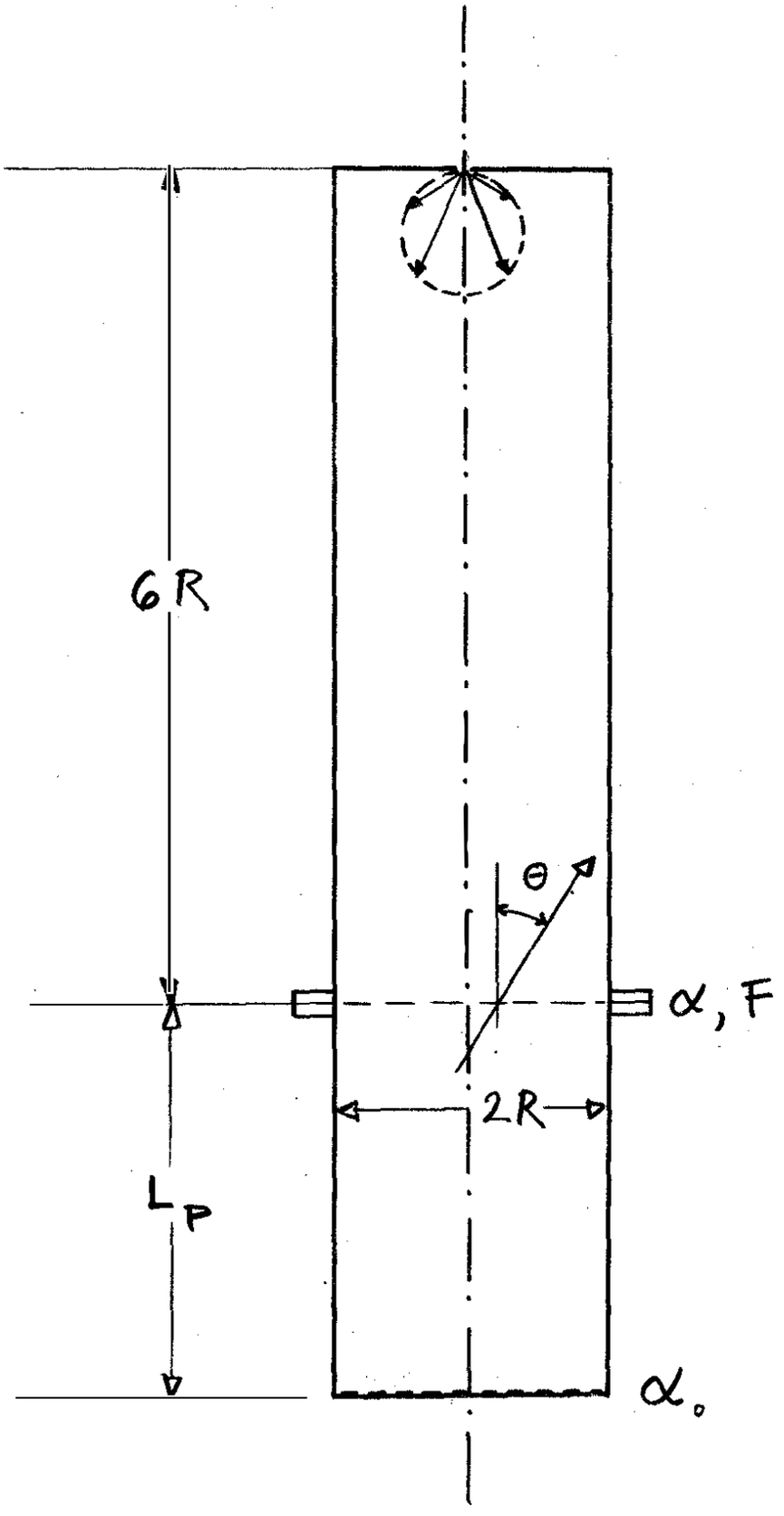

Fig. 4 Pump representation (b)

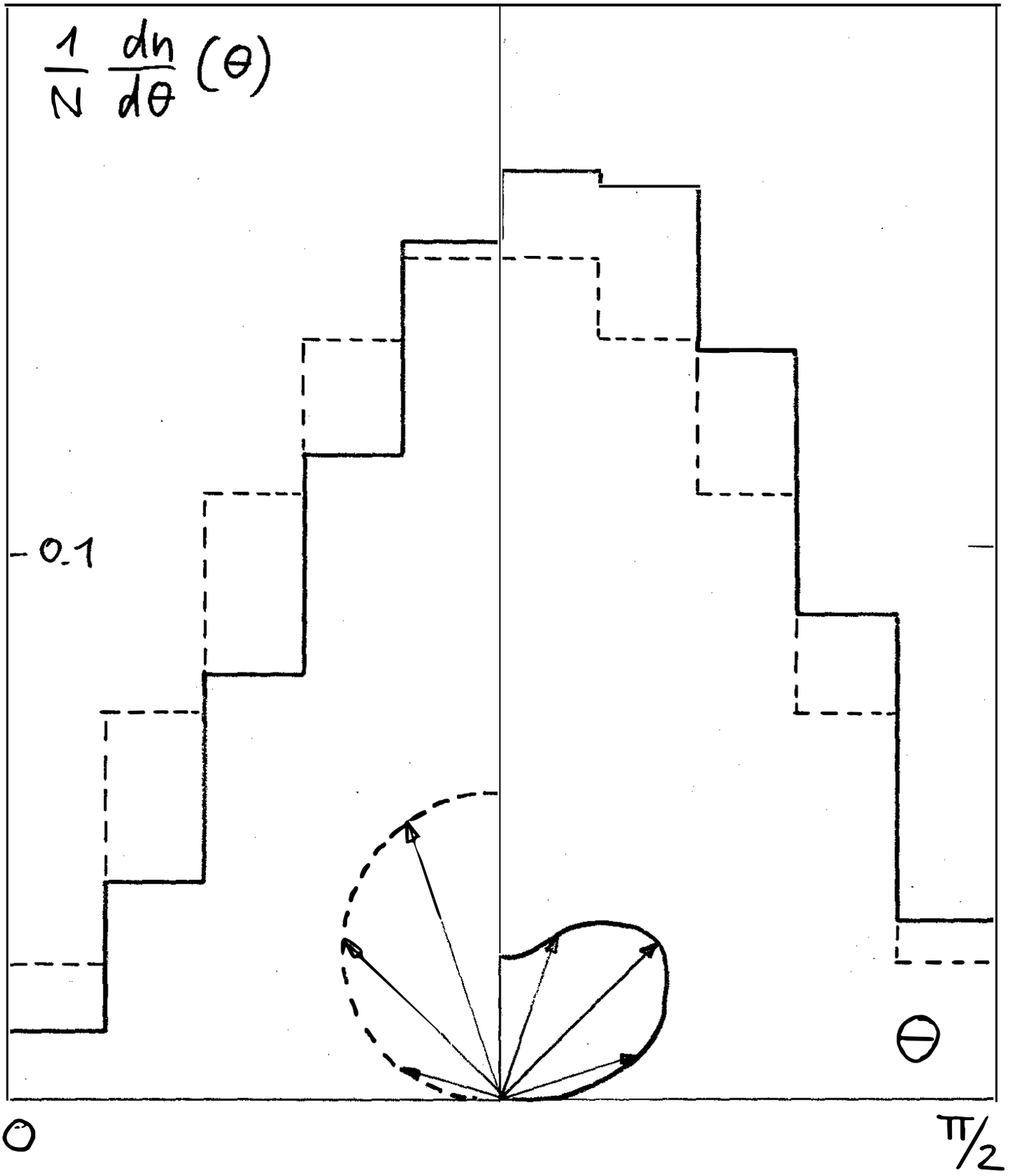

Fig. 5 Typical angular distribution of molecules reflected from the pump (F = -0.19)

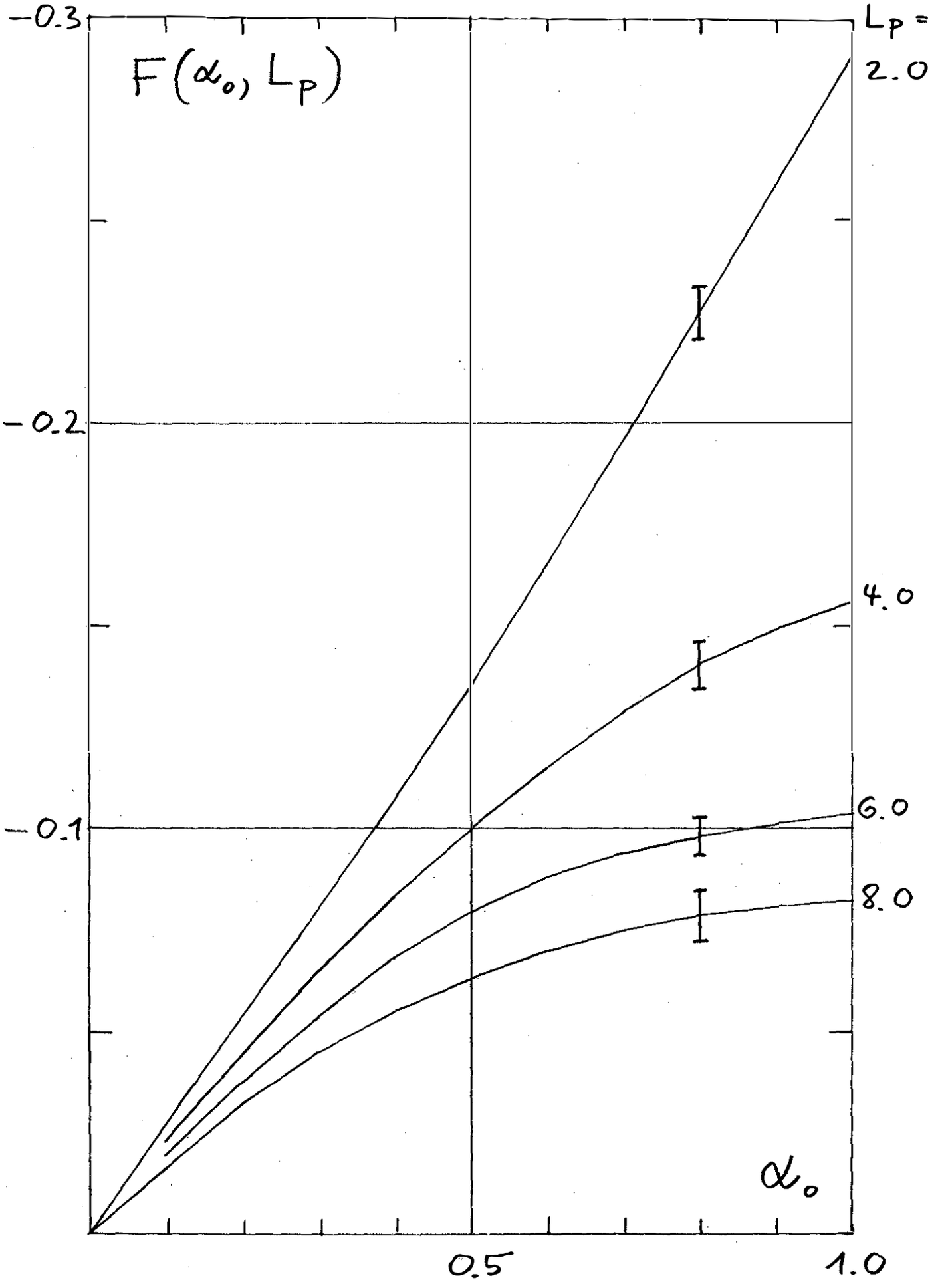

Fig. 6 Beaming factor for pump representation (b)

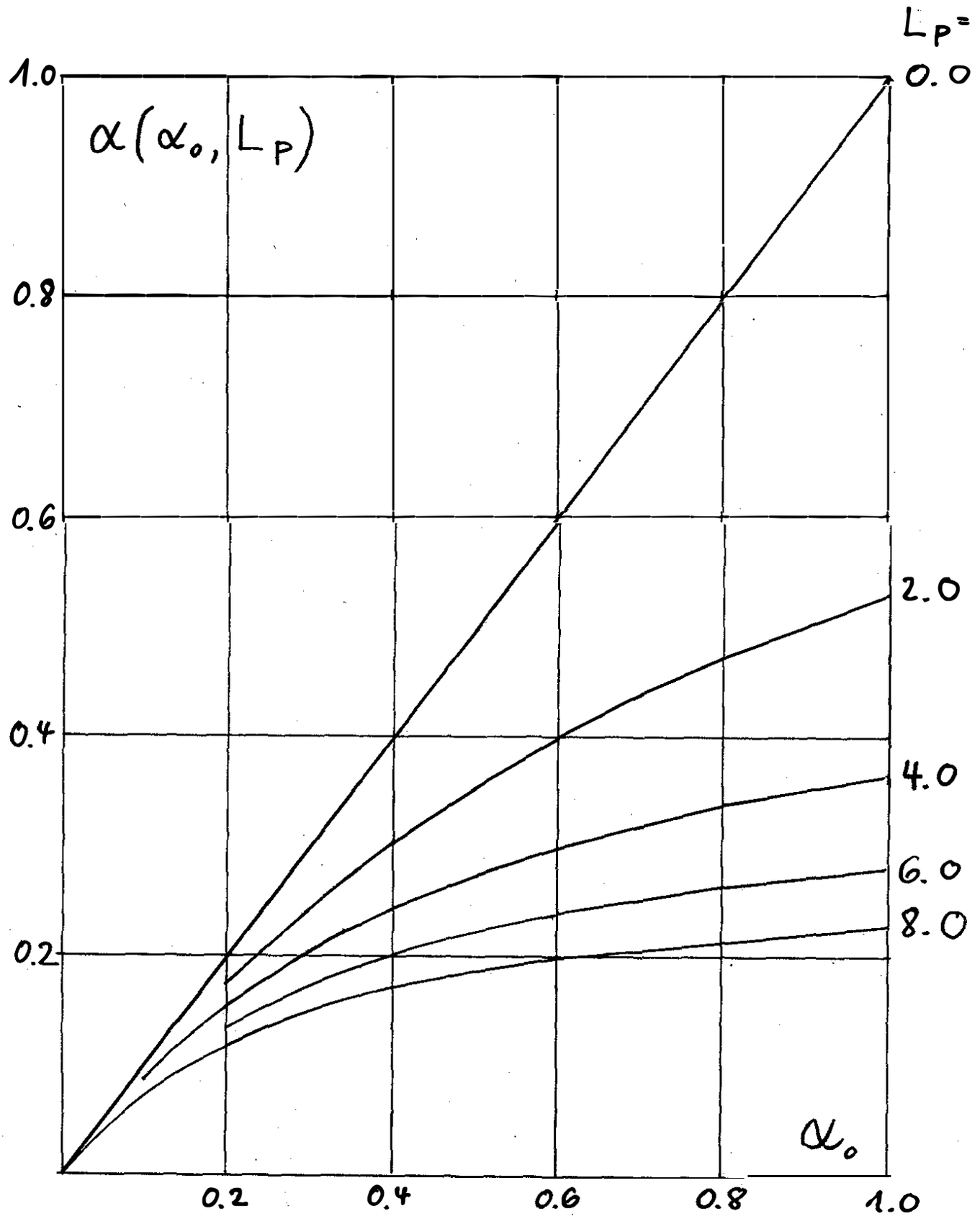

Fig. 7 Effective pumping probability for pump representation (b)

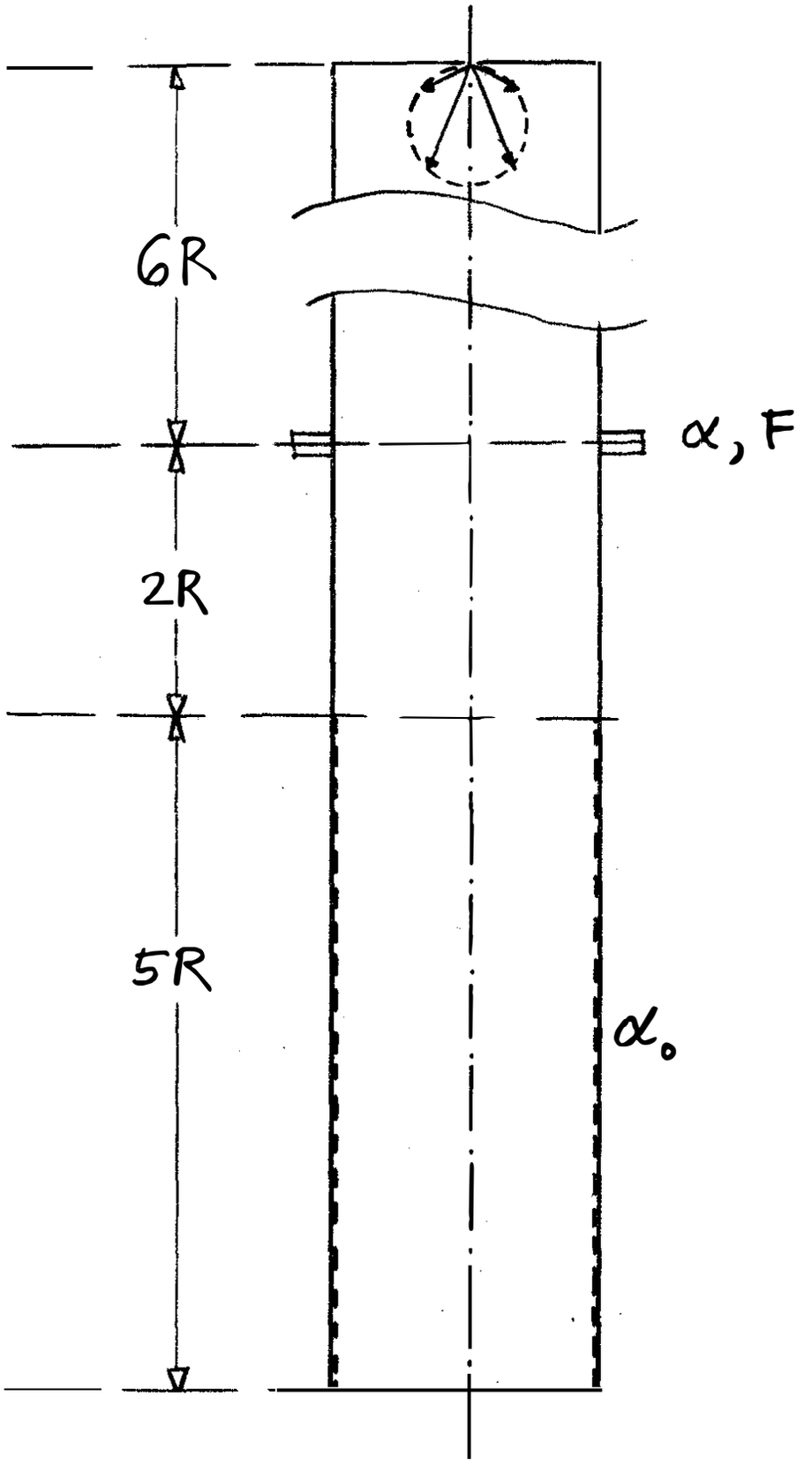

Fig. 8 Pump representation (c)

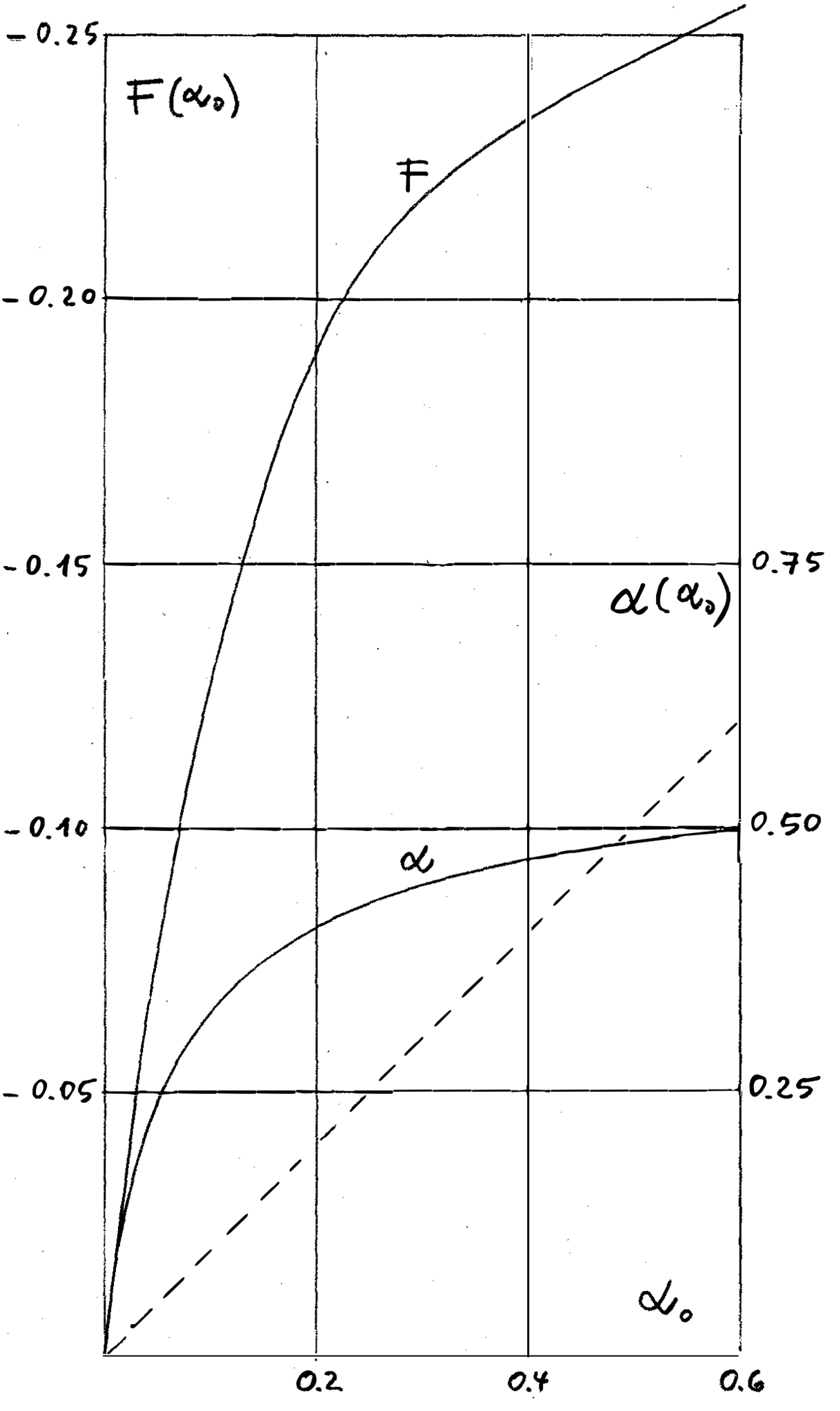

Fig. 9 Beaming factor and effective pumping probability for pump representation (c)

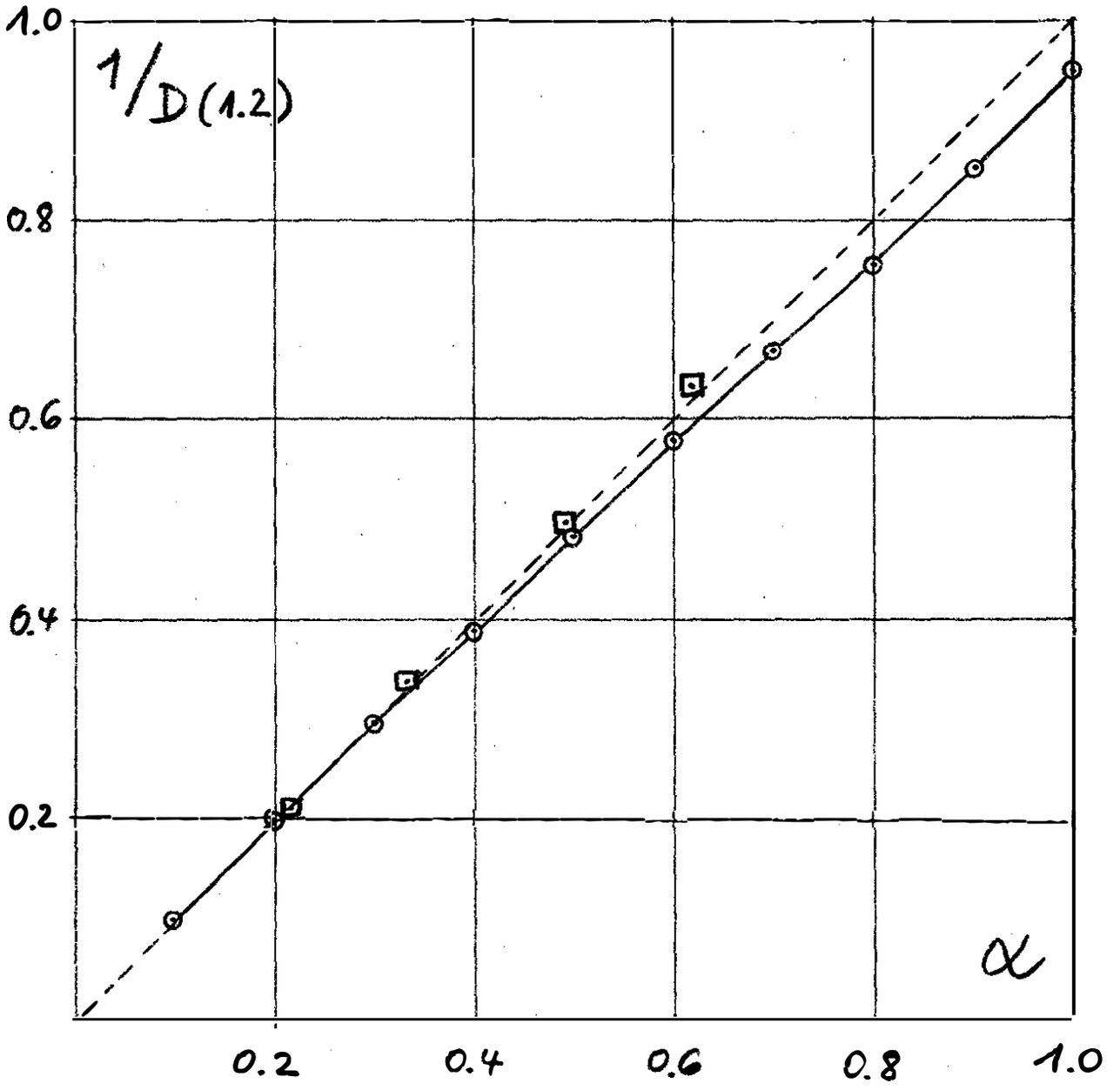

Fig. 10 Comparison of computations on the ISO test dome

⊡ J.N. Chubb

⊙ Authors